FUSED FILAMENT FABRICATION ADDITIVE MANUFACTURING: MECHANICAL RESPONSE OF POLYETHYLENE TEREPHTHALATE GLYCOL

O. Kohn[1], Y. Rosenthal[1], D. Ashkenazi[2,*], R. Shneck[3], A. Stern[1,3]

[1] School of Mechanical Engineering, Afeka Academic College of Engineering, Tel Aviv, 69107, Israel
[2] School of Mechanical Engineering, Tel Aviv University, Ramat Aviv 6997801, Israel
[3] Department of Materials Engineering, Ben-Gurion University of the Negev, Beer Sheva 8410501, Israel
*Corresponding author's e-mail address: dana@eng.tau.ac.il

ABSTRACT

The additive manufacturing (AM) fused filament fabrication (FFF) technology is widely used today with different kinds of thermoplastic materials, including polyethylene terephthalate glycol (PETG). One of the major problems of parts produced by AM-FFF technology is the anisotropy of their mechanical properties. Therefore, it is very important to understand the effect of build strategy and post-processing on the mechanical properties and failure behavior of the FFF-PETG components. This research aims to examine the influence of 3D-print orientations, post-processing heat treatments and reinforcement of the material with carbon fibers, on the mechanical properties of FFF-PETG specimens. For this purpose, three different standard building orientations, flat, one-edge and upright specimens were printed. Tensile testing was carried out to obtain the mechanical properties of the FFF-PETG specimens for the different 3D-print orientations and post-processing. The specimens were characterized by visual testing, stereo microscopy, and SEM microscopy to examine the fracture surface after tensile test. The upright-melted specimens reached the same tensile strength as the as-printed flat and on-edge orientations specimens. The fracture surface of all three orientations is brittle and it typically starts by a mirror pattern that evolves into cleavage plates.

KEYWORDS: PETG polymer, additive manufacturing, fused filament fabrication (FFF), mechanical properties, tensile test, fractography.

1. INTRODUCTION

Fused deposition modeling, formally known as fused filament fabrication (FFF), is an additive manufacturing (AM) process based on a thermoplastic filament fed into a heating chamber and extruded through the print nozzle in a prescribed manner at its melting temperature. The filament is circular in cross-section with specific diameters for each FFF system. The extruded semi-liquid material cools quickly from the melting temperature to chamber temperature, and the deposited material creates a two-dimensional layer on top of another, creating the designed three-dimensional object [1] - [3].

The nature of the FFF process offers many advantages, such as design freedom to produce complex shapes without the need to invest in expensive dies and molds, and the ability to produce internal features, which is impossible using traditional manufacturing techniques. On the other hand, FFF technology poses challenges, such as producing parts with anisotropic mechanical properties, a coarse surface finish, the staircase effect at curves, the need for supports for overhanging regions and more [1] - [3]. Since AM-FFF technique is not yet well standardized by users and manufacturers, it is difficult to safely predict the as-printed properties of the components because many parameters influence the quality of the printed part, such as print strategy, print temperature, print rate and more. To overcome these challenges, many researchers focus on refining the quality of FFF parts, including improving the mechanical properties of the printed materials [1] - [3].

The commonly used polymers for AM FFF are ABS (acrylonitrile butadiene styrene), PLA (polylactic acid) and PA (polyamide). PETG (polyethylene terephthalate glycol) is a material with many advantages that has been increasingly gaining popularity for FFF usage. It combines the consistency of PLA, in terms of printability, with the strength of ABS but deforms slightly more than ABS before failure. PETG is an amorphous polymer which is easy

Date of submission/acceptance: 22.11.2021/15.11.2021 https://doi.org/10.35219/awet.2021.06

to print, with very low crystallization levels, it has excellent chemical resistance, including high-water resistance, and the density range 1.26–1.29 g/cc [4], [5]. As an alternative FFF material, different customized parts are produced for the food industry (food-safe containers) and for medical applications (medical device packing and rigid structures to endure the sterilization process). PETG is not brittle in filament form, is a relatively tough and durable material, and is more flexible than ABS and PLA. This makes PETG a good choice when prototyping mechanical parts for structural applications, encouraging mechanical properties improvement research [6] - [10].

Many scholars focus on the mechanical properties of FFF-PETG, investigating the effect of process parameters such as specimen orientation, print strategy (infill pattern and percentage), layer height, etc. Experimental data on the mechanical properties and photomicrographs of the fracture surfaces indicate that the strength of the FFF material depends on the filament mechanical properties and intralayer/interlayer filament bond strength [1] - [3], [6] - [11].

The intralayer and interlayer strength varies with the neck size generated by the diffusion between the liquid and solid filaments during the FFF process [11]. The impact of post-processing heat treatment aimed at enhancing FFF-PETG mechanical properties has been reported in literature [12], [13]. The FFF-PETG strength can be improved by applying a post-processing heat treatment at an annealing temperature higher than the glass transition temperature, aimed to increase the neck size.

In a study by Amza et al. (2021) [12], the authors demonstrated that applying an annealing heat treatment to FFF-PETG printed parts embedded in a sodium chloride powder bed resulted in improved tensile and compressive strength. The embedding of the samples helps to evenly distribute the heat, constraining the samples to avoid deformation, and preventing thermal stress buildup inside the specimens [12]. Reinforcing FFF-PETG material with short carbon fibers (PETG+CF) has been examined and the experimental data have been recently published [4], [13] - [18]. It has been observed that the reinforced PETG+CF specimens present better mechanical properties; the ultimate tensile strength was improved by 12% and the modulus of elasticity by 29% [15], [18], [19].

The objective of the present on-going research is to investigate the mechanical properties of FFF-PETG products used for structural applications. The effect of specimen print orientation, post-processing heat treatment and reinforcement of the material with carbon fibers on the mechanical properties of FFF-PETG specimens have been investigated.

2. EXPERIMENTAL PART

2.1. Specimens

In this study the specimens were printed with Sunhokey 1.75 mm PET-G filament using an Artillery Sidewinder x1 printer; the build orientation and printing parameters are shown in figure 1 and table 1, respectively. The 3D-print parameters were defined according to the suggested values in the literature [1], [9], [20], [21]. The tensile test specimens, designed by CAD model according to ASTM D-638-14 standard, were printed in three different orientations (Fig. 1): upright - along the Z axis, on-edge – along the Y axis, flat – along the X axis. The geometry of the tensile test specimen is shown in figure 2.

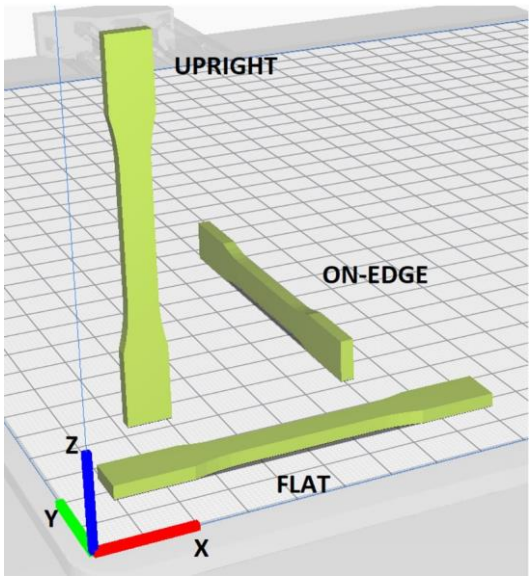

Fig. 1. The tensile test specimens CAD model showing the three test configurations: flat, on-edge, upright build orientations

Table 1. FFF-PETG printing parameters

Printing temperature	*235 °C
Platform temperature	80-90 °C
Printing speed	55 mm/min
Density	1.27 g/cm^3
Tensile strength	53 MPa (from literature)
Perimeters (walls)	1
Infill percentage	100%
Infill/raster angle	+45°/-45°
Internal infill pattern	Rectilinear
Layer Height (LH)	0.2 mm
Outline overlap	35%
Part cooling fan speed	0 RPM
First layer speed	40%, 22 mm/min

* It is common practice to print PET-G between 220-250 °C [20]

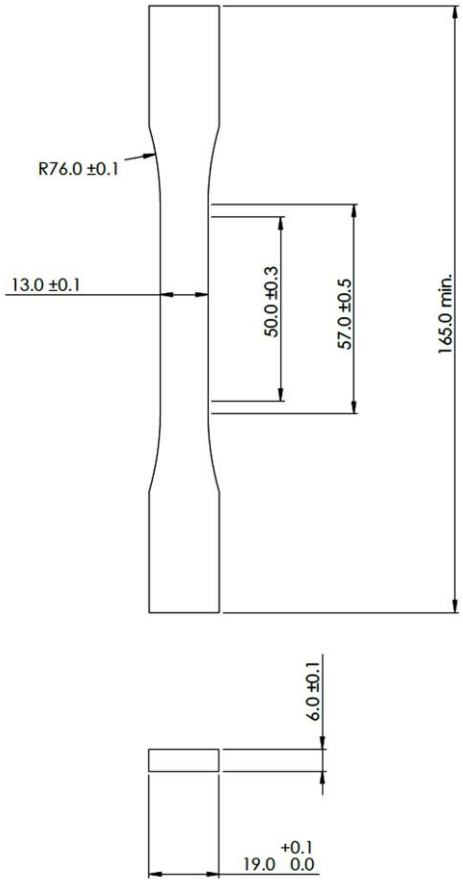

Fig. 2. The geometry of the tensile test specimen (according to ASTM D-638-14)

2.2. Tensile Testing

Tensile tests were conducted with a computerized Tinius Olsen H25KT universal testing machine using a crosshead velocity of 0.5 mm·min^{-1}. Load and displacement were acquired on-line during the test and used to calculate and obtain all the relevant parameters, e.g., engineering stress-strain curves. The errors for the two parameters are (1) displacement with an error of 0.02 mm; and (2) load in Newtons 0.5 % error. A total of 36 specimens were tested (not including four specimens which were used for calibration), three specimens for each orientation in four configurations as follows: as-printed, closed-mold melting, carbon fiber reinforcement and annealing process.

2.3. Post Printing Processing

2.3.1. Closed-Mold Melting

A negative mold of the tensile test specimen model was manufactured (machined) from AL-6061. The test specimen was placed inside the mold; then the mold was closed and was inserted into a sand bath. Next, the specimen inside the mold surrounded by the sand bath was inserted into an oven, which was preheated to 235 °C. The specimen with the mold was heated inside the oven for two hours and the sand bath with the mold was then pulled out of the oven. There was a five-hour.

2.3.2. Annealing Heat Treatment

The same procedure was used for the annealing heat treatment; the difference between the two processes was the temperature of the oven, which was set at 135 °C; therefore, the specimens were not melted. All the other steps were similar in both processes.

2.3.3. Carbon Fiber Reinforcement

The process of carbon fiber reinforcement (fusing with carbon fibers) was similar to the closed-mold melting process. The difference between the processes was that here, a layer of carbon fiber was placed at the bottom of the mold before inserting the specimen into the mold. Aksaca Carbon Fiber A-38 (0.2 mm ±5%) was used for all the experiments. All the other steps of the process were similar.

2.4. Structure Characterization

The general properties of the FFF-PETG are summarized in Table 2 [20], [21]. Visual testing (VT) inspection combined with Nikon SMZ800 light microscopy (LM) and JEOL 5400 scanning electron microscopy (SEM) observations were performed following the mechanical testing. The quality of the printed surfaces, including possible defects, as well as the fracture surface morphology were examined. For the SEM examination the fractured surfaces were coated with a thin layer of gold.

Table 2. FFF-PETG general properties, Sunhokey filament [21]

Properties	**Typical value**	**Test method**
Material Density	1.27 g/cm^3	ASTM D1505
Yield tensile strength	53 MPa	ASTM D638
Break tensile strength	26 MPa	ASTM D638
Elongation at break	70%	ASTM D638
Flexural strength	80 MPa	ASTM D790
Flexural modulus	2150 MPa	ASTM D790
Heat distortion temperature	74 °C	ASTM D648
Vicat softening temperature	83 °C	ASTM D1525
Printing temperature	*190-220	-
Hot pad	**0-40	-

* It is common practice to print PET-G between 220-250 °C [21]

** It is common practice to heat the build platform between 80-100 °C [21]

2.5. Fractography

The fracture morphology was analyzed under a Nikon SMZ800 optical microscope at various magnifications. Examination of the fracture surfaces by a JEOL 5400 SEM revealed many new features.

3. RESULTS AND DISCUSSION

3.1. Mechanical Properties

The mechanical properties (ultimate tensile stress - UTS, elongation at UTS and at rupture) of the FFF-PETG specimens after tensile testing are reported in Table 3. The presented values are the average of the experimental results obtained for each configuration after post-processing.

Table 3. Average mechanical properties (each of three tested specimens) of the different configurations: UTS and strain at UTS and break

Sample	σ_{UTS} [MPa]	ε% at UTS	ε% at break
Flat average	46.9	2.9	4.0
On-edge average	47.4	3.1	4.3
Upright average	24.3	1.8	1.8
Flat average – Melted	29.9	2.0	2.0
On-edge average- Melted	32.5	2.1	2.1
Upright Average – Melted	40.8	2.3	2.3
Flat average- Melted - Carbon	27.0	2.2	2.2
On-edge average - Melted - Carbon	24.9	1.4	1.4
Upright Average - Melted - Carbon	24.3	1.5	1.5
Flat average - Annealed	43.2	2.4	2.4
On-edge average - Annealed	47.0	3.0	4.6
Upright average - Annealed	21.1	1.1	1.1

The stress-strain curves of the FFF-PETG as-printed materials are shown in figure 3a-c and the average mechanical properties are reported in table 3.

The stress-strain curves of the tensile FFF-PETG specimens printed according to the flat configuration for melted, melted with carbon fibers, and annealed are shown in figure 4a-c, respectively. The tensile test results presented in figure 4a-c and table 3 show that no mechanical properties improvement was achieved by applying the three types of post-processing procedures to the flat orientated specimens; both processes involving melting exhibited the lowest mechanical properties.

The stress-strain curves for the on-edge configuration and for the upright configuration for the melted, melted with carbon fibers, and annealed are shown in figure 5a-c and figure 6a-c respectively. The average mechanical properties for the three configurations after the post-processing are also summarized in table 3.

The mechanical properties presented in figure 5a-c and Table 3 for the on-edge specimens exhibit the same behavior as the flat specimens. Both post-processing processes including specimen melting produced the lowest results.

The overall mechanical performance of the melted upright specimens (Fig. 6a-c, Table 3) show that the melted specimens perform much better than the as-printed material. The other two processes did not change the properties of the printed polymer.

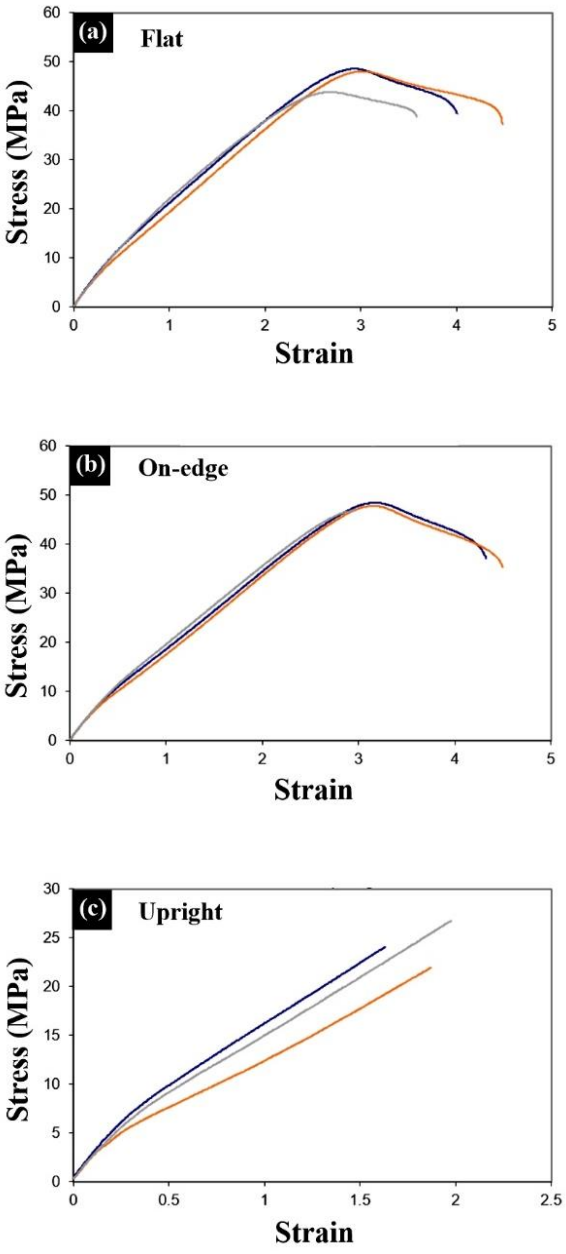

Fig. 3. The stress-strain curves of the AM FFF-PETG specimens after tensile test for the three different building orientations: (a) flat; (b) on-edge and (c) upright configurations

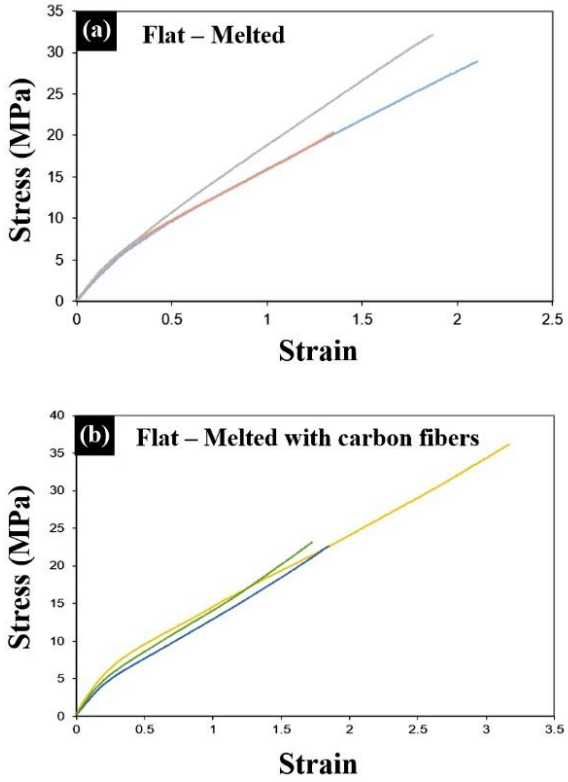

Fig. 4. The stress-strain curves of the AM FFF-PETG flat building orientation after three post-processing processes: (a) melted; (b) melted with carbon fibers; and (c) annealed

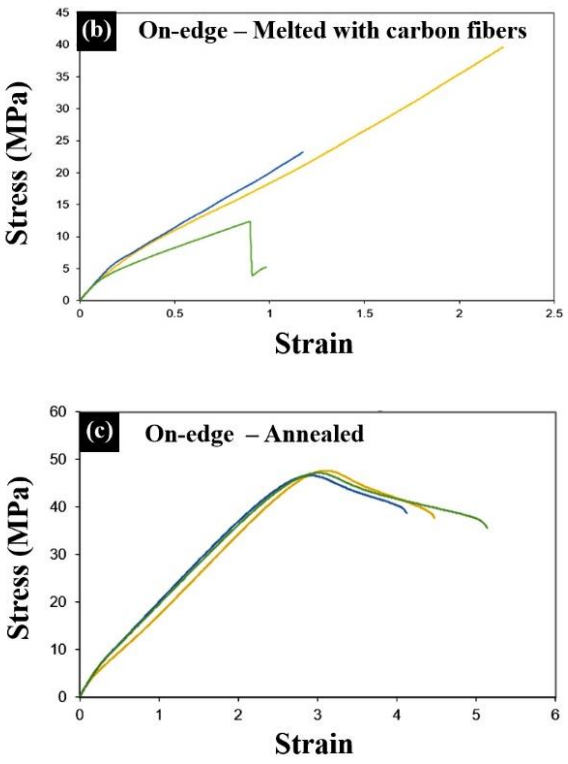

Fig. 5. The stress-strain curves of the AM FFF-PETG on-edge building orientation after three post-processing processes: (a) melted; (b) melted with carbon fibers (machine malfunctioned at specimen no.6, marked in green); (c) annealed

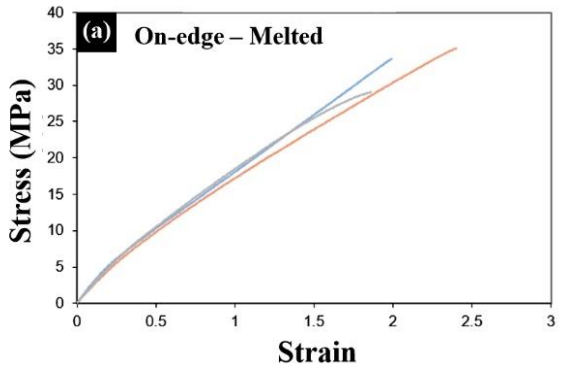

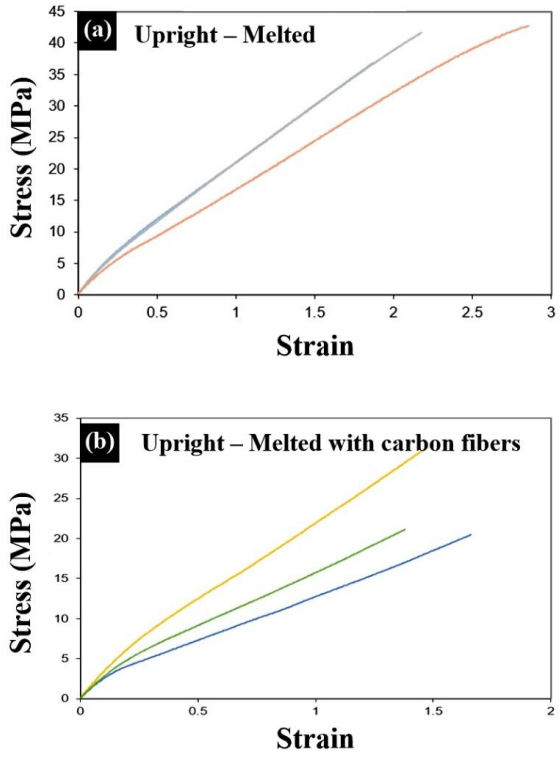

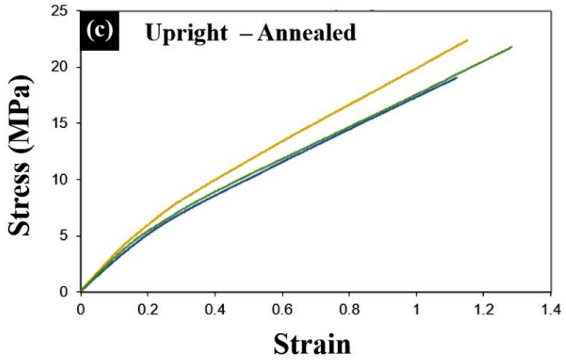

Fig. 6. The stress-strain curves of the AM FFF-PETG upright building orientation after three post-processing processes: (a) melted; (b) melted with carbon fibers and (c) annealed

3.2. Fractography

The fracture surfaces of the flat, on-edge and upright orientations are typical of brittle fractures (Figs. 7, 8 and 9, respectively, light microscope images). The fractures usually start by a mirror pattern that evolves into cleavage plates. The mirrors are centered at material defects, usually internal voids or at the free surface.

In the flat orientation, the XZ plane of the printing tray is exposed. In figure 10a (SEM image), a mosaic of wire ruptures in different directions is observed. In this specimen one can expect to encounter wires at 45º in the positive direction and 45º in the negative direction.

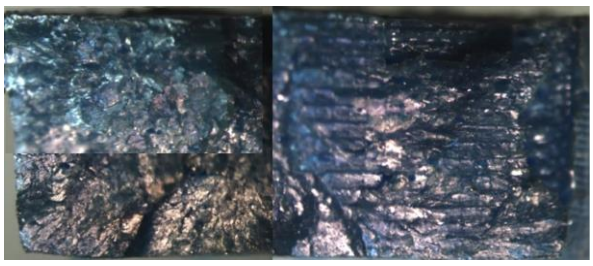

Fig. 7. The fracture surfaces of the flat orientation (LM observation)

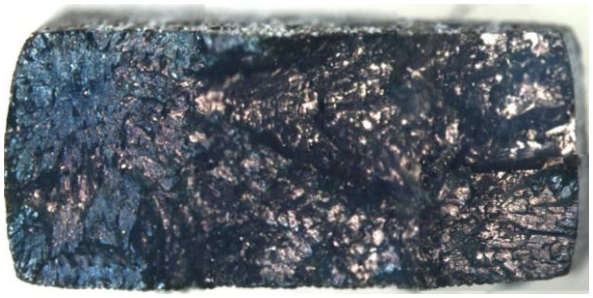

Fig. 8. The fracture surfaces of the on-edge orientation (LM observation)

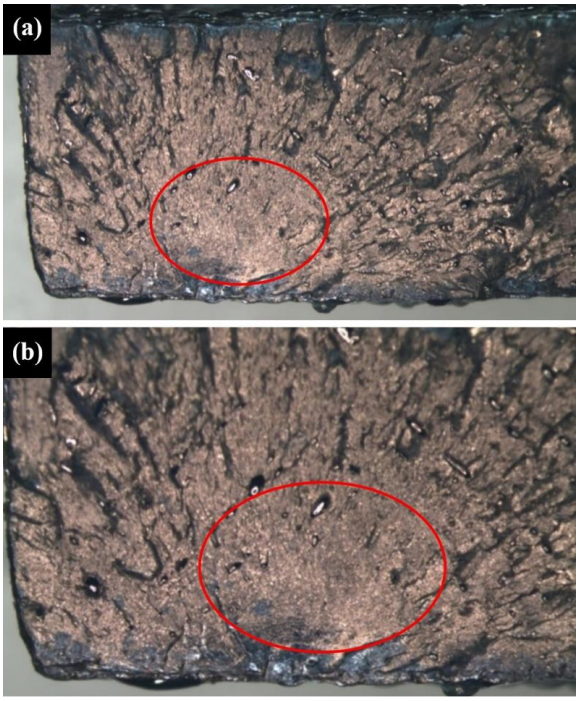

Fig. 9. The fracture surface of the upright orientation (light microscopy): (a) general view; and (b) close-up showing the crack origin

In the on-edge orientation, the YZ plane of the printing tray is exposed. In figure 10b-c (SEM images) the fracture surface is anisotropic. The various printing layers are revealed by fractures that cross wires. During the printing process, the filament coming out of the printer nozzle is semi-molten. The outer surface cools faster in a convection mechanism than the inner part of the filament, which cools in a conduction mechanism. As a result, directional solidification takes place, which may be manifested by the direction of the cleavage facets in the fracture (Fig. 10a). Also, the uneven solidification may give rise to micro-cavities, which are the main source of the fractures. Figure 10b show cavities that form between wires in the same layer, which seem to be due to early solidification or high viscosity of the wires. Figure 10c shows the result of the change of printing direction from 45º positive to 45º negative. The two-and-even printing technique imparts stronger mechanical properties to printed models. However, there is also a disadvantage to this printing method in the formation of porosity in the model volume and a weak connection between the non-conjugated layers which can be weakness in the printed material.

In figure 11a-c the fracture surface of the sample in the on-edge orientation can be seen in the YZ plane under SEM observation. The underling printing texture is not evident, but many voids are exposed. A large mirror of brittle cleavage facets appears at one edge of the fracture surface. The origin of the mirror is evidently a printing void; figure 11a, c show additional large voids that did not serve as a crack origin.

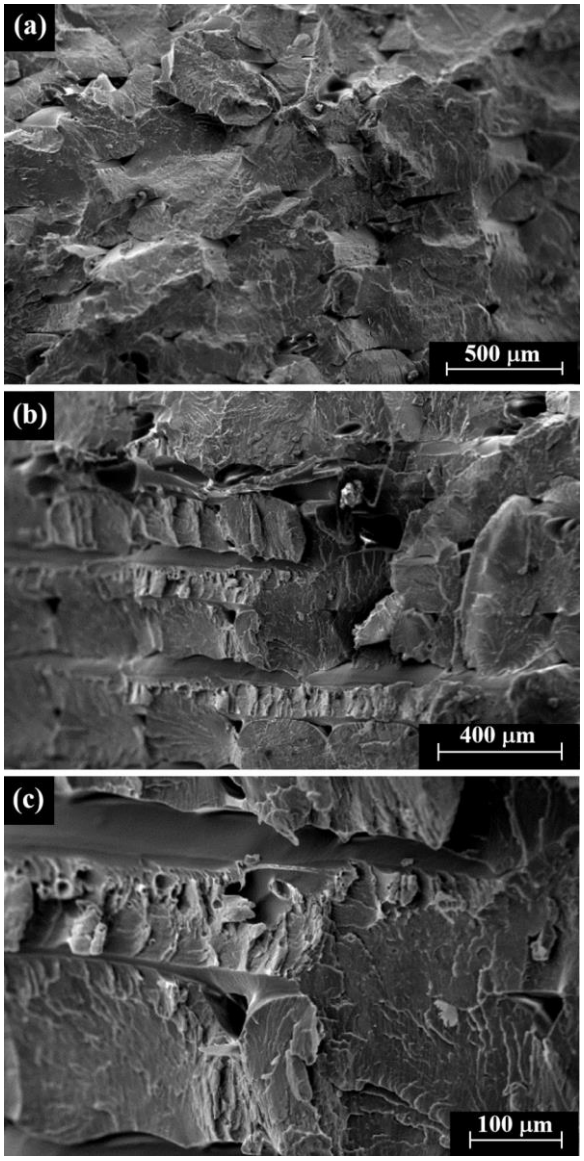

Fig. 10. SEM images of flat and on-edge fracture surfaces: (a) typical flat orientation's fracture surface, (b) and (c) typical flat and on-edge fracture orientations revealing the layered configuration of the material

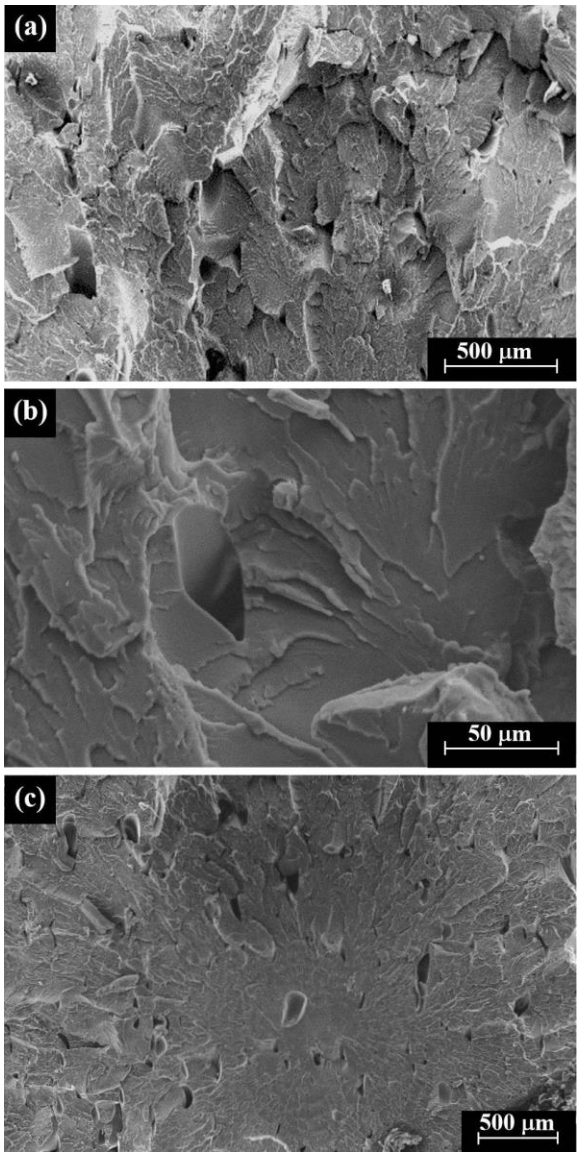

Fig. 11. SEM images of on-edge fracture surface: (a) general view of the crack propagation surface; and (b) close-up image of a typical void along the crack path; and (c) general view of the main crack origin

In figure 12 the fracture of the upright-oriented model is shown. The sample was printed in a direction perpendicular to the tensile direction; these surfaces are the weakest plane of the printed material. The underling printing texture of XY plane is not evident and the mechanical weakness appears only by the planar, brittle appearance of the fracture surface (Fig. 12b, d).

The fracture originated at a void close to the free surface. The initiation is microscopically flat and becomes rougher in figure 12c as the crack extends. Such observations are usually explained in terms of fracture mechanics. The elastic energy release rate increases with increasing crack length, and this provides enough energy to create a free surface as the crack advances.

4. CONCLUSIONS

- This study examined the influence of the AM-FFF technology orientations, post-processing heat treatments and reinforcement of the 3D-printed material with carbon fibers, on the mechanical properties of FFF-PETG tensile specimens. For that purpose, three different standard building orientations, flat, on-edge and upright specimens (Fig. 2) were printed. The FFF-PETG specimens in the three building orientations were characterized by tensile testing and the fracture surfaces of all specimens were examined.
- The tensile strength and elongation properties (Table 3) were measured in the current research because they are of particular interest for describing the stress-strain properties of polymeric materials.

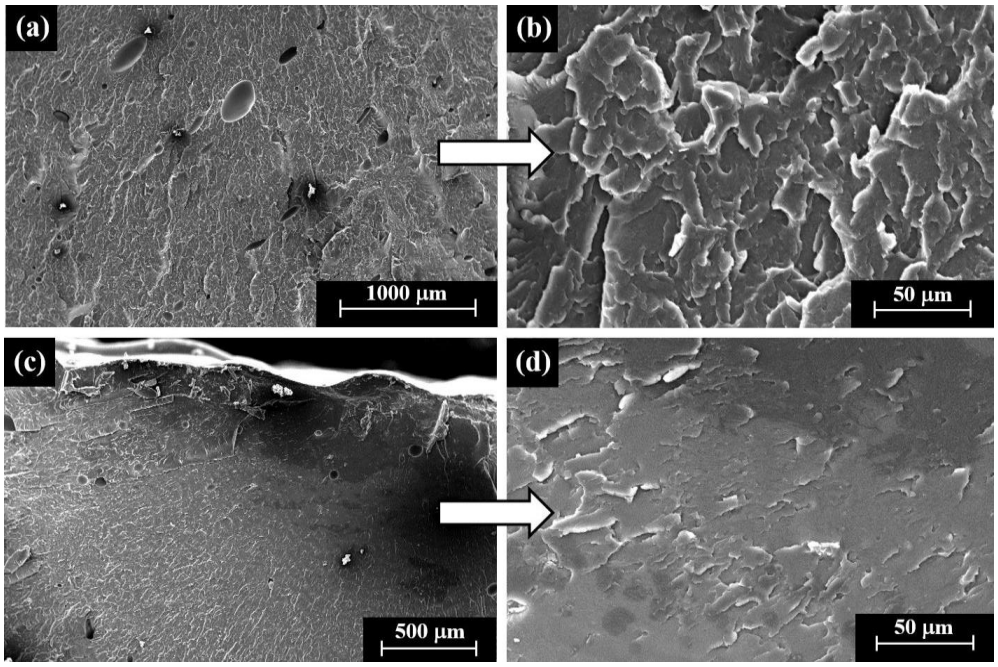

Fig. 12. SEM images of the upright fracture surface: (a) general view of crack propagation surface; (b) crack origin; (c) close-up of initial crack propagation; and (d) close-up view of crack propagation

- This study is part of an ongoing project on FFF-ABS, FFF-PLA shape memory polymer (SMP) and FFF-PETG. In a future study it is recommended to examine the influence of the annealing time and temperature on the mechanical properties of the FFF-PETG specimens. Moreover, in the next stage the fractographic study of the specimens will be performed with tools such as multifocal 3D digital light microscopy and SEM following the mechanical testing in order to further study the quality of the printed surfaces and possible correlation to the stress-strain curves. In addition, the influence of the annealing temperature and time on the mechanical properties of the FFF-PETG will be examined. We also intend to apply the nondestructive testing (NDT) micro computed tomography (micro-CT) analysis on the FFF samples. Boundary conditions and design calculations will be also included.
- The annealed specimens of the three orientations did not show any improvement of the overall mechanical properties after the heat treatment process.
- The closed mold melting upright specimens showed a notable increase in their tensile strength, whereas the on-edge and flat specimens showed a slight reduction of their tensile strength. The upright specimens returned to original strength of the polymer by re-melting.
- All the carbon fiber reinforced specimens were weakened by the process; the carbon layer created pores across the cross-sections of all specimens, weakening the material.
- The upright specimens which were melted reached the same tensile strength as the specimens printed in the flat and on-edge orientations.
- The fracture surface of the flat, on-edge and upright orientations is brittle, and it normally starts by a mirror pattern that evolves into cleavage plates.
- Based on current research results, our suggested hypothesis about the possible strengthening of the PETG specimens was correct; the upright specimens were significantly strengthened by the melting post-processing, achieving properties close to the polymer's strength.

ACKNOWLEDGEMENTS

This research was supported by Afeka Academic College of Engineering and Ben Gurion University to whom the authors are grateful. Thanks, are also due to A. Ulanov, V. Palei, S. Maman and I. Kravchinsky, Department of Mechanical Engineering, Afeka Academic College of Engineering, for their technical assistance and their students' guidance. We are thankful to the students A. Yurchenko and B. Zobok from Ben Gurion University, Department of Materials Engineering, for their permission to use and publish their projects data and results of their research. The authors are also grateful to B. Doron for the English editing.

REFERENCES

[1] **Popescu D., Zapciu A., Amza, C., Baciu, F., Marinescu, R.,** *FDM process parameters influence over the mechanical properties of polymer specimens: A review*, Polymer Testing, vol. 69, 2018, pp. 157-166.

[2] **Dizon J. R. C., Espera Jr A. H., Chen Q., Advincula R. C.**, *Mechanical characterization of 3D-printed polymers*, Additive Manufacturing 20, 2018, pp. 44–67.

[3] **Somireddy M., Czekanski A., Singh C. V.**, *Development of constitutive material model of 3D printed structure via FDM*, Materials Today Communications 15, 2018, pp. 143–152.
[4] **Kasmi S., Ginoux G., Allaoui S., Alix S.**, *Investigation of 3D printing strategy on the mechanical performance of coextruded continuous carbon fiber reinforced PETG*, Journal of Applied Polymer Science 138(37), 2021, p .50955.
[5] **Guessasma S., Belhabib S., Nouri, H.**, *Printability and tensile performance of 3D printed polyethylene terephthalate glycol using fused deposition modelling*, Polymers, 11(7), 2019, p. 1220.
[6] **Szykiedans K., Credo W., Osiński, D.**, *Selected mechanical properties of PETG 3-D prints*, Procedia Engineering 177, 2017, pp. 455–461.
[7] **De Miranda M. F. O., Ribeiro F.J.O., dos Santos Saad N., Guarato A. Z.**, *Cob-2019-1931: Experimental analysis on the mechanical properties of PETG parts made with fused deposition modeling manufacturing*, 25th ABCM International Congress of Mechanical Engineering, October 20-25, 2019, Uberlandia, MG, Brazil, pp. 1–5.
[8] **Durgashyam K., Reddy M. I., Balakrishna A., Satyanarayana K.**, *Experimental investigation on mechanical properties of PETG material processed by fused deposition modeling method*, Materials Today: Proceedings 18, 2019, pp. 2052–2059.
[9] **Srinivasan R., Ruban W., Deepanraj A., Bhuvanesh R., Bhuvanesh T.**, *Effect on infill density on mechanical properties of PETG part fabricated by fused deposition modelling*, Materials Today: Proceedings 27, 2020, pp. 1838–1842.
[10] **Panneerselvam T., Raghuraman S., Krishnan, N. V.**, *Investigating mechanical properties of 3D-printed polyethylene terephthalate glycol material under fused deposition modeling*, Journal of the Institution of Engineers (India): Series C 102(2), 2021, pp. 375–387.
[11] **Gurrala P. K., Regalla, S. P.**, *Part strength evolution with bonding between filaments in fused deposition modelling: This paper studies how coalescence of filaments contributes to the strength of final FDM part*, Virtual and Physical Prototyping 9(3), 2014, pp. 141–149.
[12] **Amza C. G., Zapciu A., Constantin G., Baciu F., Vasile M.I.**, *Enhancing mechanical properties of polymer 3D printed parts*, Polymers 13(4), 2021, p. 562.
[13] **Mansour M., Tsongas K., Tzetzis D., Antoniadis A.**, *Mechanical and dynamic behavior of fused filament fabrication 3D printed polyethylene terephthalate glycol reinforced with carbon fibers*, Polymer-Plastics Technology and Engineering 57(16), 2018, pp. 1715–1725.
[14] **Bhandari S., Lopez-Anido R. A., Gardner D. J.**, *Enhancing the interlayer tensile strength of 3D printed short carbon fiber reinforced PETG and PLA composites via annealing*, Additive Manufacturing 30, 2019, p.100922.
[15] **Kannan S., Ramamoorthy M., Sudhagar E., Gunji, B.**, *Mechanical characterization and vibrational analysis of 3D printed PETG and PETG reinforced with short carbon fiber*, AIP Conference Proceedings 2270(1), 2020, p. 030004. AIP Publishing LLC.
[16] **Sanei S. H. R., Popescu D.**, *3D-printed carbon fiber reinforced polymer composites: a systematic review*, Journal of Composites Science 4(3), 2020, p. 98.
[17] **Mahesh V., Joseph A. S., Mahesh V., Harursampath D.**, 2021. *Investigation on the mechanical properties of additively manufactured PETG composites reinforced with OMMT nanoclay and carbon fibers*, Polymer Composites 42, 2021, pp. 2380–2395.
[18] **Kichloo A. F., Raina A., Haq M. I. U., Wani, M. S.**, *Impact of carbon fiber reinforcement on mechanical and tribological behavior of 3D-printed polyethylene terephthalate glycol polymer composites—An experimental investigation*, Journal of Materials Engineering and Performance, 2021, pp. 1–18.
[19] **Kumar M. A., Khan M. S., Mishra S. B.**, *Effect of machine parameters on strength and hardness of FDM printed carbon fiber reinforced PETG thermoplastics*, Materials Today: Proceedings 27, 2020, pp. 975–983.
[20] https://all3dp.com/(accessed on 15.10.2021).
[21] https://sunhokey.cn/ (accessed on 05.10.2021).